Identification of promising drug candidates against Non-Structural Protein 15 (NSP15) from SARS-CoV-2: an *in silico* assisted drug-repurposing studies

Rameez Jabeer Khan[$,1], Rajat Kumar Jha,[$,1], Ekampreet Singh[1], Monika Jain[1], Gizachew Muluneh Amera[1], Rashmi Prabha Singh[2], Jayaraman Muthukumaran[1,*], Amit Kumar Sing[1,*]

[1]Department of Biotechnology, School of Engineering and Technology, Sharda University, P.C. 201310, Greater Noida, U.P., India

[2]Department of Biotechnology, IILM College of Engineering & Technology, Greater Noida, U.P, India

[$]Authors Contributed equally

*Correspondence authors E-mail address:

Dr. Amit Kumar Singh: amitk.singh@sharda.ac.in and

Dr. Jayaraman Muthukumaran: j.muthukumaran@sharda.ac.in

Running Title: Identification of antiviral drugs against NSP15 from SARS-CoV-2

Abstract

The recent COVID-19 pandemic caused by SARS-CoV-2 has recorded a high number of infected people across the globe. The notorious nature of the virus makes it necessary for us to identify promising therapeutic agents in a time-sensitive manner. The current study utilises an *in silico* based drug repurposing approach to identify potential drug candidates targeting non-structural protein 15 (NSP15), i.e. uridylate specific endoribonuclease of SARS-CoV-2 which plays an indispensable role in RNA processing and viral immune evasion from the host immune system. NSP15 was screened against an in-house library of 123 antiviral drugs obtained from the Drug Bank database from which three promising drug candidates were identified based on their estimated free energy of binding (ΔG), estimated inhibition constant (*Ki*), the orientation of drug molecules in the active site and the key interacting residues of NSP15. The MD simulations were performed for the selected NSP15-drug complexes along with free protein to mimic on their physiological state. The binding free energies of the selected NSP15-drug complexes were also calculated using the trajectories of MD simulations of NSP15-drug complexes through MM/PBSA (Molecular Mechanics with Poisson-Boltzmann and surface area solvation) approach where NSP15-Simeprevir (-242.559 kJ/mol) and NSP15-Paritaprevir (-149.557 kJ/mol) exhibited the strongest binding affinities. Together with the results of molecular docking, global dynamics, essential dynamics and binding free energy analysis, we propose that Simeprevir and Paritaprevir are promising drug candidates for the inhibition of NSP15 and could act as potential therapeutic agents against SARS-CoV-2.

Keywords: Drug repurposing, SARS-CoV-2, NSP15, Molecular Docking, MD simulation, MM/PBSA

Abbreviations: NSP15: Non-Structural Protein15; MD: Molecular Dynamics; RMSD: Root Mean Square Deviation; RMSF: Root Mean Square Fluctuation; Rg: Radius of Gyration; SASA: Solvent Accessible Surface Area; PCA: Principal Component Analysis; ED: Essential Dynamics

1. Introduction

Coronaviruses of the coronaviridae family are enveloped, non-segmented, positive-sense RNA viruses which poses an unusually large genome ranging from 24 kb to 32 kb consisting of a unique replication strategy [1]. They are known etiological agents in mammals and birds, causing respiratory, enteric, hepatic and neurologic diseases [2]. Two coronaviruses, namely SARS-CoV and MERS-CoV, have been the cause to epidemics in 2002 and 2010 [3], respectively. The COVID-19 pandemic caused by SARS-CoV-2 originated in Wuhan, China, in December 2019 and has now expanded to over 180 countries infecting more than 6 million people and causing 370,000+ mortalities [4]. The highly contagious nature of the virus makes it crucial for researchers to identify inhibitory methods against this pathogen.

In our study, we propose non-structural protein 15 (NSP15), uridylate specific endoribonuclease, as a potential druggable target due to its essential role in the viral life cycle [5]. NSP15 is a unique molecular marker for Nidovirales that aids in the processing of both ssRNA and dsRNA by preferentially cleaving 3' of uridylates generating a 2',3' cyclic phosphate and 5'-OH using Mn^{2+} as a cofactor for its activity [6]. The catalytic activity of NSP15 is conferred by its *C* terminal domain containing the active site residues responsible for uridylate specificity for cleavage [7]. Structural studies of NSP15 reveal that it assembles into a double ring hexamer which is essential for enzymatic activity and is known to be cooperatively stabilised by monomeric interactions which makes it sensitive to mutations and small molecules which can disrupt the oligomeric assembly [8]. Mutational studies of the catalytic site show reduced sub genomic RNA accumulation and attenuation of viral infection [9, 10]. NSP15 has been found to inhibit the activity of mitochondrial antiviral signalling adaptor as a method of immune evasion [11]. NSP15 lacking endoribonuclease activity stimulated an early induction of cytosolic dsRNA, causing intense activation of type I interferons (IFN-1) and Protein Kinase R (PKR) mediated apoptosis, exhibiting an impaired viral growth [6].

Moreover, NSP15 plays a crucial role in RNA processing and viral immune evasion from the host immune system, which shows that it plays an essential role in the viral life cycle. The present study employs a systematic computer-aided drug repurposing approaches to identify the promising drug molecules from an in-house antiviral library with the help of molecular docking and MD simulations include analysis of global dynamics, essential dynamics and binding free energy analysis. The molecules obtained from the present study are showing strong binding affinity and significant structural stability towards NSP15.

2 Material and Methods

2.1 Receptor preparation

The three-dimensional crystal structure of NSP15 from SARS-CoV-2 was downloaded from Research Collaboratory Structural Bioinformatics - Protein Data Bank (RCSB-PDB) [12] using the accession number of 6W01 [13]. After downloading the structure from PDB, the model was cleaned up by excluding the water molecules and heteroatoms. Upon cleaning up the structure, energy minimisation was performed using YASARA web server [14]. The structural evaluation was accomplished using Structure Analysis and Verification Server (SAVES) v5.0 (https://servicesn.mbi.ucla.edu/SAVES/) (UCLA MBI), which incorporate three programs namely ERRAT [15], Verify-3D [16] and ProCheck [17] programmes.

2.2 Screening of antiviral drugs against NSP15

For virtual screening, an in-house library of one hundred twenty-three antiviral drugs (see supplementary data) were used. The antiviral drug library was prepared by manually downloading antiviral drugs in structure data file (SDF) format from the Drug Bank [18] database. The PyRx v0.8 (https://pyrx.sourceforge.io/downloads) was the software of choice for virtual screening and molecular docking. It utilises the Auto Dock Vina [19] program for performing the molecular docking studies between the protein and ligand molecules. Since the catalytic site residues of NSP15 were already known, site-specific docking or direct docking (Grid Box: Center_x = -64.60 Å, Center_y = 68.57 Å, Center_z = 31.84 Å, Size_x = 25.00 Å, Size_y = 22.89 Å, Size_z = 23.93 Å) was performed for its screening against the antiviral drug library. During the screening and molecular docking operation, exhaustiveness was set to 32 to increase the probability of detecting the global minimum of the scoring function inbuilt in Auto Dock Vina. From the results obtained from virtual screening, the best three NSP15-drug complexes were selected based on estimated binding free energy (ΔG), estimated inhibition constant (Ki), their orientation at the catalytic site and the key interacting residues. These complexes were subjected to molecular dynamics (MD) simulations and binding free energy analysis for understanding the structural stability and structural integrity at long intervals in the presence of an aqueous environment.

2.3 Molecular Dynamics (MD) Simulation

MD simulations of the free protein and the best protein-drug complexes were performed in an explicit solvent model to mimic the physiological state of protein molecules. GROMACS 2019 [20] was employed to perform MD simulations using GROMOS96 43a1 [21] force field parameters, and PRODRG [22] webserver was used to generate the topology of drug

molecules. The MD simulations were run for a proceeding of 100 ns for the protein and protein-drug complexes. Counter ions (positive or negative) were added to the complexes to make the system electrostatically neutral. Solvation of the complexes was performed within a 10 Å SPC/E water cube [23]**.** The detailed protocol of MD simulation has already been discussed in our previous publication [24].

2.4 Binding Free Energy Calculations

In order to understand how the drug molecules were interacting and behaving with NSP15 at long intervals, we extracted the complexes every 1 ns from the global trajectories of 100 ns MD simulations and subjected them to Molecular Mechanics with Poisson–Boltzmann and Surface area Solvation (MM/PBSA) binding free energy analyses. In this analysis, we calculated the binding free energies of the three most promising NSP15-drug complexes.MM/PBSA is one of the most preferred end-state methods to calculate the binding free energies of protein-ligand complexes [25]. It can be calculated via the following equation:

$$\Delta G_{binding} = G_{Complex} - [G_{Protein} + G_{Ligand}]$$

Here, $\Delta G_{binding}$ represents the binding free energy of the protein-ligand complexes, $G_{Complex}$ represents the total free energy of the same protein-ligand complex, and $G_{Protein}$ and G_{Ligand} represent the total free energies of the protein and ligand molecule. The binding free energies of the promising NSP15-drug complexes were performed using the *g_mmpbsa* [26] tool.

3.Results and Discussion

3.1 Structural analysis of NSP15

The functional NSP15 is a hexamer comprised of a dimer of trimers. Each monomer consists of three domains, the *N* terminal domain (residues 1-62) followed by a central middle domain (residues 63-191) and the catalytic *C* terminal domain (residues 192-345) with its edge hosting the catalytic site. The catalytic site is in a shallow groove consisted of six highly conserved residues, namely His235, His250, Lys290, Thr341, Tyr343, and Ser294. These key active site residues are conserved among SARS-CoV, MERS-CoV and SARS-CoV-2. Based on a similar arrangement with RNase-A, His235, His250, Lys290 are hypothesised to be the catalytic triad. Based on the same assumption, Ser294 and Tyr343 are proposed to confer uridylate specificity to the enzyme [8].

3.2 Virtual screening results

The top three antiviral drugs obtained from the virtual screening were Simeprevir (DrugBank ID: DB06290), Paritaprevir (DrugBank ID: DB09297) and Artesunate (DrugBank ID: DB09274). All three selected drug molecules exhibited appreciable binding affinities (ΔG > -7.0 kcal/mol) towards NSP15. Besides, all drug molecules appeared to be optimally oriented at the catalytic site of NSP15. The estimated binding energies (*ΔG*), estimated inhibition constants (*Ki*), molecular formulae and chemical schemes have been described in **Table 1**.

Table 1: Selected drug molecules obtained from virtual screening of NSP15 against the in-house library of antiviral drugs

S/No	Drug Bank ID	EBE (kcal/mol)	EIC (μM)	Molecular formula	Chemical scheme
1.	Simeprevir (DB06290)	-8.4	0.696	$C_{38}H_{47}N_5O_7S_2$	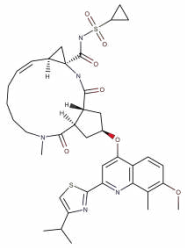
2.	Paritaprevir (DB09297)	-7.5	3.179	$C_{40}H_{43}N_7O_7S$	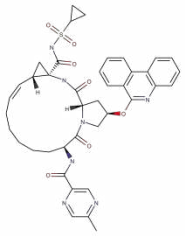
3.	Artesunate (DB09274)	-7.2	5.275	$C_{19}H_{28}O_8$	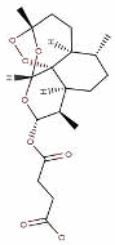

3.2.1. NSP15-Simeprevir Complex

The estimated binding free energy (*ΔG*) and the estimated inhibition constant (*Ki*) for NSP15-Simeprevir complex were -8.4 kcal/mol and 0.696 μM, respectively. The drug molecule was involved in H-bonding interactions with NSP15 via three catalytically conserved residues, namely His235, Lys290 and Thr341. Simeprevir was also found to be interacting with Met219, Ala232, His235, Asp240 and His243 utilising π interactions. Moreover, the drug molecule was also observed to be interacting with Glu234, Gly239, Phe241, Gly247, His250, Trp333, Val339, Glu340 and Tyr343 via van der Waals interactions.

3.2.2. NSP15-Artesunate Complex

The estimated *ΔG* of NSP15-Artesunate complex was -7.2 kcal/mol, and the estimated *Ki* was 5.275 μM. Artesunate was found to be interacting with NSP15 catalytic site residues via four H-bonds. The participating residues included Lys290, Ser294, Thr341 and Tyr343. Additionally, His250, His235 and Trp333 were observed to be involved in π interactions with the drug molecule. The catalytic site residues including Gly247, Gly248, Val292, Cys293, Glu340 and Lys345 were involved in Van der Waals interactions with Artesunate.

3.2.3. NSP15-Paritaprevir Complex

The estimated *ΔG* for NSP15-Paritaprevir complex was observed to be -7.5 kcal/mol, and the estimated *Ki* was 3.179 μM. Paritaprevir was observed to be interacting with NSP15 via four H-bonding interactions. The four H-bonded residues were His235, His243, Lys290 and Glu340. Also, the drug was involved in π interactions with Ala232 and His235. Van der Waals interactions also contributed to the binding of Paritaprevir to NSP15. The drug interacted with Glu234, Asp240, Gln245, Leu246, Gly248, Val339 and Thr341 residues via Van der Waals interactions.

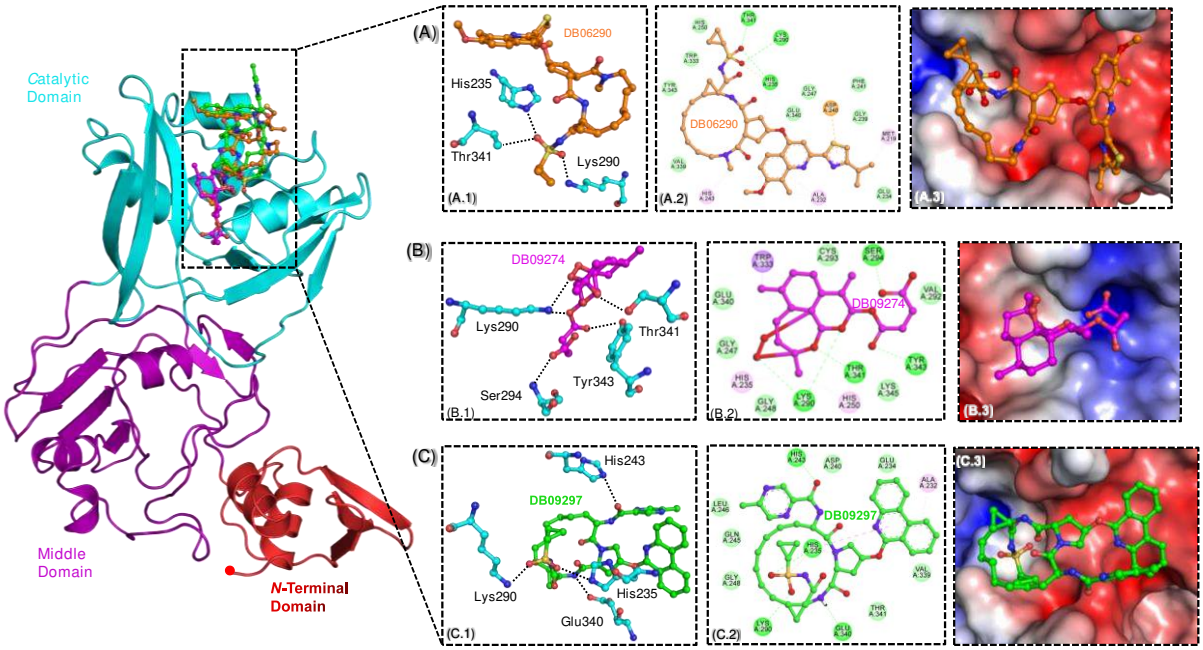

Fig. 1 Interaction of three promising drug molecules with NSP15 (A) Three-Dimensional (3D) (A.1), Two-Dimensional (2D) (A.2) and Electrostatic (A.3) surface representation of NSP15 active site residues interacting with Simeprevir (DrugBank ID: DB06290) (Orange) (B) 3D (B.1), 2D (B.2) and Electrostatic (B.3) surface representation of NSP15 active site residues interacting with Artesunate (DrugBank ID: DB09274) (Magenta) (C) 3D (C.1), 2D (C.2) and Electrostatic (C.3) surface representation of NSP15 active site residues interacting with Paritaprevir (DrugBank ID: DB09297) (Green) [2D Figure info: van der Waals interactions (slightly green colour), hydrogen bonds (dark green colour), and pi-interactions (light pink colour)]

All the intermolecular interactions have been summarised in **Table 2**. As evident from the binding pattern analysis, all three drugs exhibited extensive interactions with the conserved catalytic site residues with $\Delta G > 7.1$ kcal/mol and $Ki < 5.3$ µM. According to the binding free energy values, the order of drugs showing the most potent interactions towards NSP15 was Simeprevir > Paritaprevir > Artesunate. In terms of intermolecular interactions, all three drug molecules exhibited a minimum of three H-bonds towards NSP15. Additionally, Simeprevir and Paritaprevir share a very similar cyclic backbone, and it could be a reason why both drugs were among the top hits of virtual screening.

Table2. Interaction details of Simeprevir, Paritaprevir and Artesunate with NSP15

Hydrogen Bond residues (HB), Distance (D), Pi-Interaction Sharing Residues (Pi-SR), and van der Waals Interaction Sharing Residues (vdWISR)

3.3 MD Simulations of selected NSP15-drug complexes

Molecular docking does not take the dynamic behaviour of protein molecules into

S/No	DrugBank ID	HB	D (Å)	Pi-SR	D (Å)	vdWISR
1.	Simeprevir (DB06290)	His235 Lys290 Thr341	1.98 2.07 2.63	Met219 Ala232 His235 Asp240 His243	4.82 4.21, 4.89 4.51, 5.42 3.37 5.10	Glu234, Gly239, Phe241, Gly247, His250, Trp333, Val339, Glu340, Tyr343
2.	Paritaprevir (DB09297)	His235 His243 Lys290 Glu340	2.63 2.63 2.55 2.06	Ala232 His235	4.12 3.87 5.33 5.42	Glu234, Asp240, Gln245, Leu246, Gly248, Val339, Thr341
3.	Artesunate (DB09274)	Lys290 Ser294 Thr341 Tyr343	2.12, 5.89 1.79 2.75 2.49	His250 His235 Trp333	4.92 4.52, 4.92 3.91, 6.55	Gly247, Gly248, Val292, Cys293, Glu340, Lys345

account [27], which makes it physiologically less relevant than MD simulations. MD simulations of 100 ns were performed to study the dynamic behaviour of NSP15 and its drug bound complexes. MD simulations were utilised to calculate various time-averaged structural parameters including RMSD (Root Mean Square Deviations), RMSF (Root Mean Square Fluctuations), Rg (Radius of Gyration), SASA (Solvent Accessible Surface Area) and intermolecular hydrogen bonding. The trace of the covariance matrix was also obtained from PCA (Principal component analysis) based on the ED (Essential dynamics) approach, which only considers the biologically relevant motions.

3.3.1 Root Mean Square Deviations (RMSD)

RMSD analysis elucidates the structural deviations of entire protein molecules with respect to time. The time-averaged RMSD values of free NSP15, NSP15-Simeprevir, NSP15-Artesunate and NSP15-Paritaprevir were calculated to be 0.366 nm, 0.525 nm, 0.715 nm, and 0.390 nm, respectively. The results showed that the drug bound NSP15 complexes were deviating more than the native protein. The average deviations were insignificant in the case

of NSP15-Paritaprevir, but they increased significantly in the case of NSP15-Simeprevir and NSP15-Artesunate. **Fig. 2(a)** illustrates the graph of RMSD values of NSP15 and its drug bound complexes with respect to time. Out of all three drug molecules, Paritaprevir induced least structural deviations in NSP15 in comparison to the free protein. Simeprevir induced higher average deviations than the free NSP15 throughout the MD simulation, but it was also observed stabilising NSP15 after 40 ns. Finally, Artesunate was the most destabilising drug amongst all as it induced maximum structural deviations in NSP15 throughout the 100 ns of MD simulation.

3.3.2 Root Mean Square Fluctuations (RMSF)

RMSF analysis explains the residual fluctuations in a protein molecule. It was calculated for the $C\alpha$ atom of each amino acid residue of NSP15 and its drug bound complexes. The average RMSF values of free NSP15, NSP15-Simeprevir, NSP15-Artesunate and NSP15-Paritaprevir were calculated to be 0.198 nm, 0.257 nm, 0.290 nm, and 0.223 nm, respectively. The average RMSF values explicated that the binding of drug molecules did not significantly perturb the fluctuations of individual residues of NSP15. **Fig. 2(b)** showcases the graph of the fluctuations of individual residues of NSP15 and its drug bound complexes. The random fluctuations spanned the entire structure, notably the *N*-terminal domain. Interestingly, the residues of NSP15 between 15-85 residues projected the least fluctuations even though the loops dominate this segment. Majority of the peaks in the RMSF graph were observed for NSP15-Artesunate complex, and the amino acid residues of remaining NSP15-drug complexes remained remarkably stable. For all the NSP15-drug complexes except NSP15-Artesunate, the RMSF rarely crossed 3 Å, which depicted high complex stability.

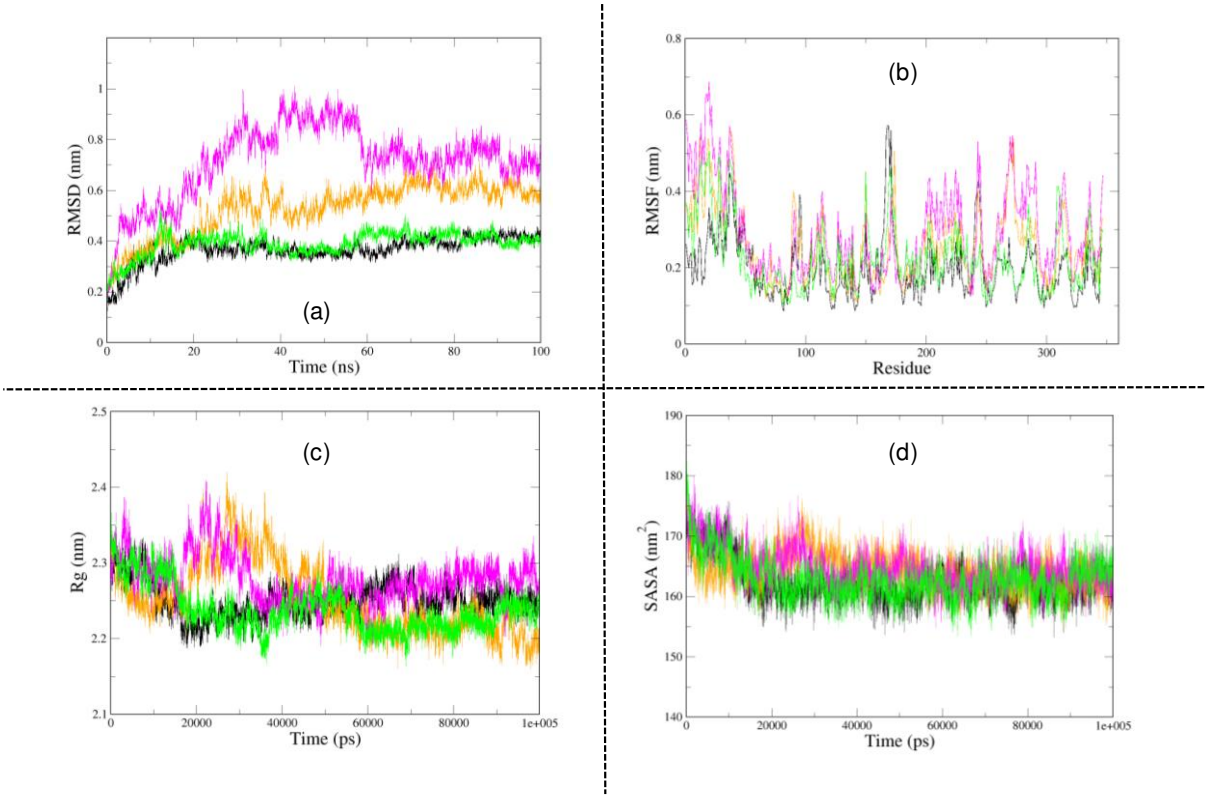

Fig. 2 Analysis of Molecular Dynamics Simulation results of free NSP15 (Black), NSP15-Simeprevir complex (Orange), NSP15-Artesunate complex (Magenta) and NSP15-Paritaprevir (Green) (a) Root Mean Square Deviation (RMSD) (b) Root Mean Square Fluctuation (RMSF) (c) Radius of Gyration (Rg) (d) Solvent Accessible Surface Area (SASA)

3.3.3 Radius of gyration (Rg)

Rg elucidates the folding nature, spatial arrangement, and denseness of protein molecules. The time-averaged Rg values of free NSP15, NSP15-Simeprevir, NSP15-Artesunate and NSP15-Paritaprevir were measured to be 2.250 nm, 2.252 nm, 2.278 nm, and 2.237 nm, respectively. **Fig. 2(c)** showcases the graph of Rg values of NSP15 and its drug bound complexes with respect to time. Artesunate was observed to be perturbing the folding characteristics and compactness of NSP15 the most, even though the absolute disturbances were minimal. The data revealed that the drug molecules only marginally altered the folding characteristics of NSP15, which suggested high stability of NSP15-drug complexes.

3.3.4 Solvent accessible surface area (SASA)

SASA can be applied to assess the alterations in the solvent behaviour of protein molecules. It was computed to examine the disturbances in the solvent behaviour of drug bound NSP15 complexes in comparison to the native protein. The time-averaged SASA values of free NSP15, NSP15-Simeprevir, NSP15-Artesunate and NSP15-Paritaprevir were measured to be

162.34 nm², 164.35 nm², 164.69 nm² and 162.85 nm², respectively. **Fig. 2(d)** showcases the graph of SASA of NSP15 and its drug bound complexes with respect to time. All three drug molecules induced an increase in SASA, which could have resulted from the solvent exposure of a few of the internal residues. However, the variations in the SASA were mostly insignificant, suggesting structural integrity of NSP15-drug complexes.

3.3.5 Intermolecular hydrogen bonding

Intermolecular H-bonds were computed to assess the stability of NSP15-drug complexes. It is one of the most significant non-covalent interactions through which a ligand could interact with the protein molecule. The time-averaged intermolecular H-bonds between NSP15-Simeprevir, NSP15-Artesunate and NSP15-Paritaprevir were recorded to be 2, 1 and 2, respectively. **Fig. 3(a)** illustrates the graph of H-bonds between NSP15 and bound drugs with respect to time. The time-averaged values suggested that, except Artesunate, all other drug molecules interacted appreciably with NSP15.

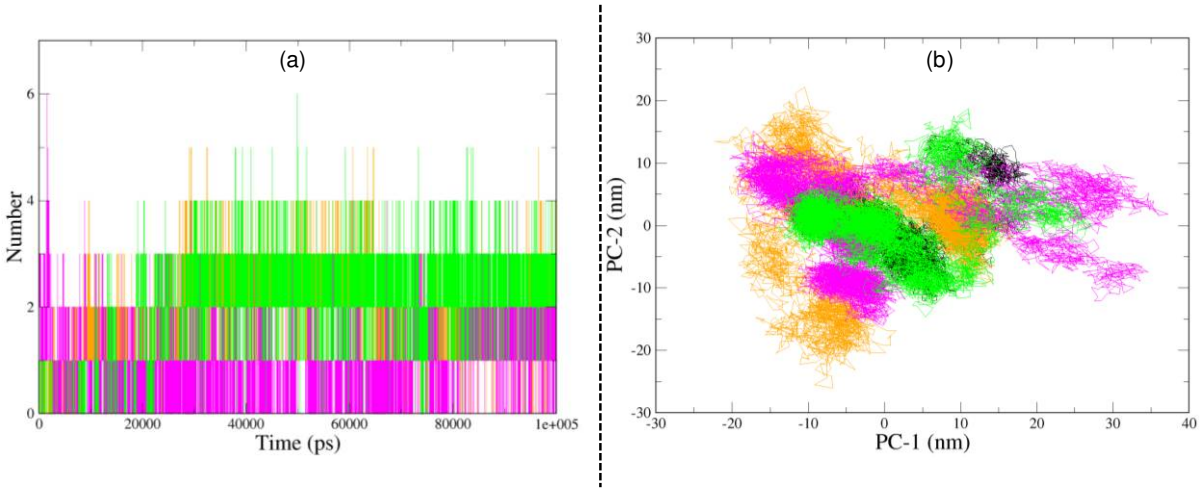

Fig. 3 Analysis of Molecular Dynamics Simulation results of free NSP15 (Black), NSP15-Simeprevir complex (Orange), NSP15-Artesunate complex (Magenta) and NSP15-Paritaprevir (Green) (a) Intermolecular H-bonds (b) Principal component analysis.

3.3.6 Principal component analysis (PCA)

Generally, a protein molecule achieves its function through the collective motion of its atoms**,** and therefore these atomic motions are widely used to assess the conformational stability of protein-ligand complexes. PCA was performed to reveal the essential motions from the global trajectories of NSP15 and its drug bound complexes. ED was employed to capture the essential motions into two eigenvectors, namely principal component 1 (PC1) and principal component 2 (PC2). These variables represented the majority of essential *Cα* atomic

fluctuations observed during the MD simulations. **Fig. 3(b)** represents the conformational sampling of native NSP15 and its drug bound complexes in the essential subspace along both eigenvectors (PC1 and PC2). The PCA graph was plotted by projecting *Cα* atoms conferring tertiary conformations along with both principal components. The trace of covariance matrix eigenvalues for the free NSP15, NSP15-Simeprevir, NSP15-Artesunate and NSP15-Paritaprevir were measured to be 171.813 nm², 286.936 nm², 361.554 nm² and 221.161 nm², respectively. The data suggested that all the NSP15-drug complexes experienced increased structural dynamics and occupied a greater conformational subspace than the native protein. In conclusion, the PCA suggested that all the NSP15-drug complexes, particularly NSP15-Paritaprevir and NSP15-Simeprevir, were stable, and they exhibited higher conformational fluctuations than native NSP15.

3.4 Binding free energy calculation of NSP15-drug complexes

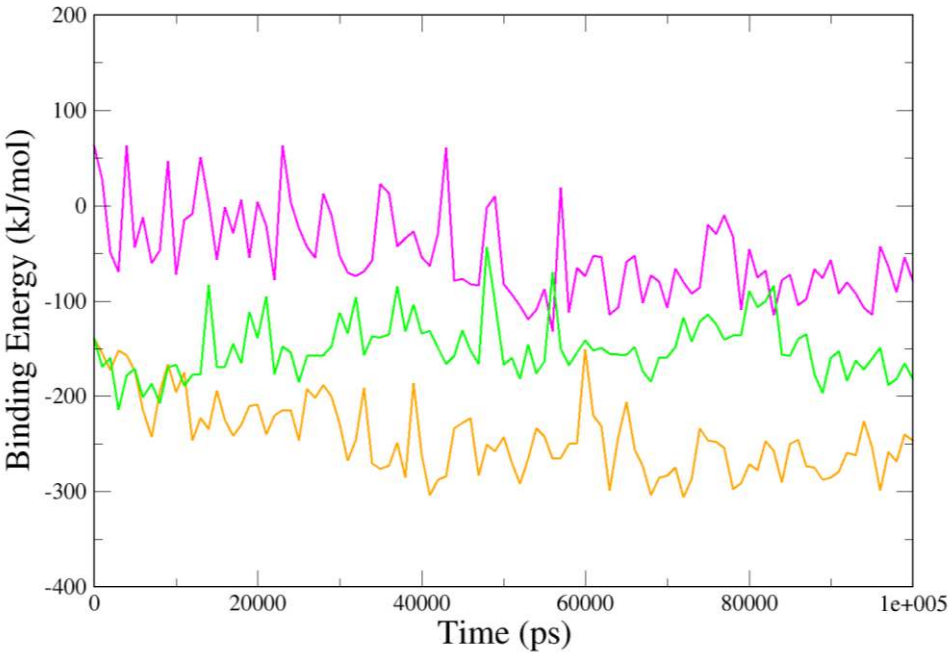

Fig. 4 Binding free energy analysis results of NSP15-Simeprevir complex (Orange), NSP15-Artesunate complex (Magenta) and NSP15-Paritaprevir (Green).

The binding free energies of NSP15-drug complexes were computed utilising MM/PBSA approach. The *g_mmpbsa* tool sampled the MD simulation trajectories of each of the complexes every 1 ns for binding free energy calculations. The binding free energies for NSP15-Simeprevir, NSP15-Artesunate and NSP15-Paritaprevir were estimated to be -242.559 kJ/mol, -51.283 kJ/mol and -149.557 kJ/mol, respectively. However, when the binding free energy of NSP15-Artesunate was calculated for the first time, the value came out to be slightly

positive (144.036 kJ/mol). To overcome this issue, the default value of the dielectric constant of the solute was adjusted from 2 to 10 in the molecular dynamics parameters file (.mdp file). After modifying the .mdp file, the binding free energy of NSP15-Artesunate was recalculated, and this time the value came out to be negative (-51.283 kJ/mol). Upon the literature survey, we found multiple supporting studies employing a similar approach to optimise the binding free energy values [28, 29]. Upon analysing individual energy components, we found that Van der Waals energies and electrostatic energies were the top contributors to the binding free energy. Conversely, polar solvation energy adversely impacted the binding free energies of all three NSP15-drug complexes.

Table 3. Contribution of individual energy components involved in complex formation between NSP15 and the top inhibitors.

S.No	System	Van der Waals energy (kJ/mol)	Electrostatic energy (kJ/mol)	Polar solvation energy (kJ/mol)	SASA energy (kJ/mol)	Binding energy (kJ/mol)
1.	NSP15-Simeprevir	-312.771	-32.482	126.732	-24.038	-242.559
2.	NSP15-Artesunate	-158.660	40.976	80.075	-13.675	-51.283
3.	NSP15-Paritaprevir	-211.531	-50.740	130.629	-17.915	-149.557

In summary, the data suggested that Simeprevir and Paritaprevir exhibited strong binding interactions towards NSP15, whereas Artesunate exhibited average interactions towards NSP15. Together with the results obtained from virtual screening, global dynamics and essential dynamics and binding free energy analyses, we propose that Paritaprevir and Simeprevir are potential inhibitors of NSP15 and are worth further *in vitro* and *in vivo* examinations. Interestingly, as discussed in our previously published study [24], Paritaprevir was found to be one of the most promising potential inhibitors of SARS-CoV-2 main protease (3CLpro). However, further experimental investigations are required to assess the inhibitory activity of Paritaprevir against either of these viral targets.

Acknowledgements

Dr. Amit Kumar Singh thanks the Department of Science and Technology (DST) and Indian National Science Academy (INSA), New Delhi, India. Gizachew Muluneh Amera thanks the College of Natural Science, Wollo University, Dessie, Ethiopia for the sponsorship.

request

References

[1] Lu, R., Zhao, X., Li, J., Niu, P., Yang, B., Wu, H., et al. Genomic characterisation and epidemiology of 2019 novel coronavirus: implications for virus origins and receptor binding. The Lancet. 395 (10224) (2020) 565-74.
[2] de Wilde, A.H., Snijder, E.J., Kikkert, M., van Hemert, M.J. Host Factors in Coronavirus Replication. In: Roles of Host Gene and Non-coding RNA Expression in Virus Infection, Tripp, R.A., Tompkins, S.M. Eds., Springer International Publishing, Cham, 2018, pp. 1-42.
[3] Zhu, N., Zhang, D., Wang, W., Li, X., Yang, B., Song, J., et al. A Novel Coronavirus from Patients with Pneumonia in China, 2019. N. Engl. J. Med. 382 (2020) 727-33.
[4] CSSE, J.H. Coronavirus COVID-19 global cases by Johns Hopkins CSSE. 2020.
[5] Zhang, L., Li, L., Yan, L., Ming, Z., Jia, Z., Lou, Z., et al. Structural and Biochemical Characterisation of Endoribonuclease Nsp15 Encoded by Middle East Respiratory Syndrome Coronavirus. J. Virol. 92 (22) (2018) e00893-18.
[6] Yanglin, Q., Kai, X. Functional studies of the coronavirus non-structural proteins. STEMedicine. 1 (2) (2020) e39.
[7] Bhardwaj, K., Palaninathan, S., Alcantara, J.M.O., Li Yi, L., Guarino, L., Sacchettini, J.C., et al. Structural and Functional Analyses of the Severe Acute Respiratory Syndrome Coronavirus Endoribonuclease Nsp15. J. Biol. 283 (6) (2008) 3655-64.
[8] Kim, Y., Jedrzejczak, R., Maltseva, N.I., Wilamowski, M., Endres, M., Godzik, A., et al. Crystal structure of Nsp15 endoribonuclease NendoU from SARS-CoV-2. Protein Sci. (2020) 1-10.
[9] Posthuma, C.C., Nedialkova, D.D., Zevenhoven-Dobbe, J.C., Blokhuis, J.H., Gorbalenya, A.E., Snijder, E.J. Site-Directed Mutagenesis of the Nidovirus Replicative Endoribonuclease NendoU Exerts Pleiotropic Effects on the Arterivirus Life Cycle. J. Virol. 80 (4) (2006) 1653-61.
[10] Kang, H., Bhardwaj, K., Li, Y., Palaninathan, S., Sacchettini, J., Guarino, L., et al. Biochemical and Genetic Analyses of Murine Hepatitis Virus Nsp15 Endoribonuclease. J. Virol. 81 (24) (2007) 13587-97.
[11] Lei, Y., Moore, C.B., Liesman, R.M., O'Connor, B.P., Bergstralh, D.T., Chen, Z.J., et al. MAVS-mediated apoptosis and its inhibition by viral proteins. PloS one. 4 (5) (2009) e5466.
[12] Berman, H.M., Westbrook, J., Feng, Z., Gilliland, G., Bhat, T.N., Weissig, H., et al. The Protein Data Bank. Nucleic Acids Res. 28 (1) (2000) 235-42.
[13] Kim, Y., Jedrzejczak, R., Maltseva, N.I., Wilamowski, M., Endres, M., Godzik, A., et al. Crystal structure of Nsp15 endoribonuclease NendoU from SARS-CoV-2. Protein Sci. (2020)
[14] Krieger, E., Joo, K., Lee, J., Lee, J., Raman, S., Thompson, J., et al. Improving physical realism, stereochemistry, and side-chain accuracy in homology modeling: Four approaches that performed well in CASP8. Proteins. 77 (Suppl 9) (2009) 114-22.
[15] Colovos, C., Yeates, T.O. Verification of protein structures: patterns of nonbonded atomic interactions. Protein Sci. 2 (9) (1993) 1511-9.

[16] Eisenberg, D., Lüthy, R., Bowie, J.U. [20] VERIFY3D: Assessment of protein models with three-dimensional profiles. In: Methods in Enzymology, Academic Press, 1997, Vol. 277, pp. 396-404.
[17] Laskowski, R.A., MacArthur, M.W., Moss, D.S., Thornton, J.M. PROCHECK: a program to check the stereochemical quality of protein structures. J. Mol. Biol. 264 (3) (1993) 283-91.
[18] Wishart, D.S., Feunang, Y.D., Guo, A.C., Lo, E.J., Marcu, A., Grant, J.R., et al. DrugBank 5.0: a major update to the DrugBank database for 2018. Nucleic Acids Res. 46 (D1) (2018) D1074-d82.
[19] Trott, O., Olson, A.J. AutoDock Vina: improving the speed and accuracy of docking with a new scoring function, efficient optimisation, and multithreading. J Comput Chem. 31 (2) (2010) 455-61.
[20] Van Der Spoel, D., Lindahl, E., Hess, B., Groenhof, G., Mark, A.E., Berendsen, H.J. GROMACS: fast, flexible, and free. J Comput Chem. 26 (16) (2005) 1701-18.
[21] Pol-Fachin, L., Fernandes, C.L., Verli, H. GROMOS96 43a1 performance on the characterisation of glycoprotein conformational ensembles through molecular dynamics simulations. Carbohydrate Res. 344 (4) (2009) 491-500.
[22] Schüttelkopf, A.W., van Aalten, D.M. PRODRG: a tool for high-throughput crystallography of protein-ligand complexes. Acta crystallographica. Section D, Biological crystallography. 60 (Pt8) (2004) 1355-63.
[23] Mark, P., Nilsson, L. Structure and Dynamics of the TIP3P, SPC, and SPC/E Water Models at 298 K. J. Phys. Chem. A. 105 (43) (2001) 9954–9960.
[24] Khan, R.J., Jha, R.K., Amera, G.M., Jain, M., Singh, E., Pathak, A., et al. Targeting SARS-CoV-2: a systematic drug repurposing approach to identify promising inhibitors against 3C-like proteinase and 2′-O-ribose methyltransferase. J. Biomol. Struct. Dyn. (2020) 1-14.
[25] Genheden, S., Ryde, U. The MM/PBSA and MM/GBSA methods to estimate ligand-binding affinities. Expert Opin Drug Discov. 10 (5) (2015) 449-61.
[26] Kumari, R., Kumar, R., Lynn, A. g_mmpbsa--a GROMACS tool for high-throughput MM-PBSA calculations. J. Chem. Inf. Model. 54 (7) (2014) 1951-62.
[27] Hollingsworth, S.A., Dror, R.O. Molecular Dynamics Simulation for All. Neuron. 99 (6) (2018) 1129-43.
[28] Ren, W., Truong, T.M., Ai, H.W. Study of the Binding Energies between Unnatural Amino Acids and Engineered Orthogonal Tyrosyl-tRNA Synthetases. Sci. Rep. 5 (2015) 12632.
[29] Martins, L.C., Torres, P.H.M., de Oliveira, R.B., Pascutti, P.G., Cino, E.A., Ferreira, R.S. Investigation of the binding mode of a novel cruzain inhibitor by docking, molecular dynamics, ab initio and MM/PBSA calculations. J. Comput. Aided. Mol. Des. 32 (5) (2018) 591-605.